Acta Materialia 110 (2016) 53–60

Contents lists available at ScienceDirect

Acta Materialia

journal homepage: www.elsevier.com/locate/actamat

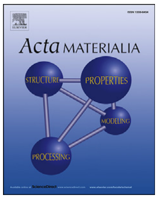

Full length article

Phase transformation during Cu_2ZnSnS_4 synthesis by reactive magnetron co-sputtering

Pierre-Antoine Cormier [a, *], Rony Snyders [a, b, **]

[a] Chimie des Interactions Plasma-Surface, Université de Mons, 23 Place du Parc, 7000, Mons, Belgium
[b] Materia Nova R & D Center, Avenue Copernic 1, Mons, Belgium

ARTICLE INFO

Article history:
Received 18 January 2016
Received in revised form
1 March 2016
Accepted 3 March 2016

Keywords:
CZTS
Reactive magnetron sputtering
Phase transformation
Phase diagram

ABSTRACT

In this work we report on the relationship between the phase constitution and the chemical composition of Cu_2ZnSnS_4 (CZTS) thin films synthesized by reactive magnetron co-sputtering of a zinc and a copper-tin alloy targets in reactive Ar–H_2S atmospheres. In order to modify the film composition, the power applied to the alloy target was modified, while the other experimental parameters were kept constant. Based on previous works, the phase constitution of the films was determined by combining multi-wavelengths Raman spectroscopy and X-Ray diffraction analysis. In our experimental window, three sets of materials are grown. The main factor determining the phase constitution was identified to be the atomic sulfur concentration in the films. Indeed, an over-stoichiometry of sulfur (<50%) was found to be necessary to synthesize CZTS films. It was shown that its decrease, associated with the increase of the Sn content lead to the disappearance of CZTS for the benefit of SnS. Based on these data, a phase diagram is built. Finally, the electrical properties of the films were evaluated by Hall effect measurements. All films exhibit a p-type conductivity with a high hole concentration between 10^{+17} and 10^{+20}. The CZTS like films present the highest carrier concentration which was explained by the presence of ZnS secondary phase. A relatively low Hall mobility was found, and explained by the small grain size (30–50 nm).

1. Introduction

Cu_2ZnSnS_4 (CZTS) is a quaternary semi-conductor that has attracted significant attention from the scientific community since several years [1,2]. Indeed, this p-type material exhibits interesting optical properties such as an optimal optical band-gap of 1.5 eV and an absorption coefficient of 10^4 cm^{-1} in the visible range [1]. According to the well-known Shokley–Queisser limit, these latter should lead to a theoretical efficiency of around 30% for CZTS based solar cells [3]. Moreover, CZTS is composed by abundant and non-toxic elements compared to conventional indium and gallium-based semiconductors (CIGS and CIS) or cadmium and tellurium-based semiconductors (CdTe) which are nowadays commonly used in solar cells.

CZTS thin films are usually synthesized by using a two-steps process: (i) the deposition of metallic precursors which can be achieved by vacuum (magnetron sputtering [4–6] or evaporation [7,8]), by wet chemistry (hydrazine-based liquid process [9]) or pulsed laser deposition [10]; and (ii) an annealing of these precursors at high temperature in sulfur atmosphere (S_2 or H_2S). Even if these techniques provided CZTS solar cells with relatively good performances (record efficiency of 9.2% [11]), their industrial transfer for large scale applications is made non optimal by the required two steps. In addition, an important drawback of these techniques is the difficulty to precisely control the film stoichiometry due to the annealing step. Indeed, a decrease of the Zn and Sn concentrations can be observed after the annealing procedure because of the evaporation of elemental Zn and of tin sulfide (SnS) that occur due to their high vapor pressures [4,7]. More specifically, the mechanisms inducing the loss of tin had been extensively studied and it is suggested that the evaporation of SnS is driven by two stages chemical reaction [12,13]: (i) the CZTS is decomposed in $Cu_2S(s)$, $ZnS(s)$, $SnS(s)$ and $S(_2g)$ and (ii) $SnS(s)$ is vaporized and desorbs. This phenomenon can be reduced by providing an excess concentration of sulfur during the growth of the film [13].

The control of the stoichiometry is, in fact, the main issue during

---

* Corresponding author.
** Corresponding author. Chimie des Interactions Plasma-Surface, Universite de Mons, 23 Place du Parc, 7000, Mons, Belgium.
E-mail addresses: pierre-antoine.cormier@umons.ac.be (P.-A. Cormier), rony.snyders@umons.ac.be (R. Snyders).

http://dx.doi.org/10.1016/j.actamat.2016.03.009
1359-6454/

the synthesis of CZTS, because it determines the phase constitution of the film which influences ultimately the performance of the solar cell [14,15]. In addition, the type of defects present in CZTS matrices is also governed by the stoichiometry of the film [16]. It has been showed that a Cu poor and Zn rich composition would be the one allowing the best power conversion efficiency [1]. It is therefore important to describe how the phase constitution of the CZTS films evolves as a function of the chemical composition of the material.

It exists several representations of this phase diagram from data related to two-steps synthesized films. For example, Oleksyuk et al. built a phase diagram of the Cu_2S–ZnS–SnS_2 pseudo-ternary system from the synthesis of 210 alloys with different Cu, Zn, Sn and S concentrations at 400 °C [14]. Their results showed that: (i) the region related to stoichiometric CZTS was very narrow and, (ii) that a small shift from the stoichiometric concentrations leads to the formation of secondary phases such as $Cu_{2-x}S$, Cu_xSnS_y or ZnS. Even if this diagram gives a clear indication over the stability of CZTS, the evolution of the phase constitution is presented according to the concentration of the Cu_2S, ZnS and SnS_2 secondary phases making difficult its use in processes where each element are modified at the same time. Platzer-Bjorkman [15] adapted this diagram by representing the phase constitution of the film before and after annealing according to the concentration of metal species (Cu, Zn and Sn). Even if this type of diagram is easier to handle, any clear quantification of the sulfur concentration in the films was given although it is a key parameter in the determination of the phase constitution. It is therefore necessary to improve this approach.

In a previous work, we have demonstrated that reactive magnetron co-sputtering was a potential alternative for the synthesis of crystallized CZTS thin films [17]. In this work a CuSn alloy (Cu/Sn = 2) and a Zn targets were co-sputtered in Ar–H_2S atmospheres while the growth temperature was >400 °C. It has been shown that the chemical composition strongly influences the crystalline structure of the deposited material, especially the copper and sulfur concentrations.

In the present work, we propose to extend and to rationalize the study of the impact of the chemical composition on the phase constitution of reactively sputtered CZTS films. In comparison with the previous work, two additional CuSn targets with Cu/Sn = 1.5 and Cu/Sn = 1 were used. The varied parameter was the power applied to the CuSn target. Each film was characterized by multi-wavelengths Raman spectroscopy (785 and 325 nm), by X-Ray Diffraction (XRD), and by Energy-dispersive X-ray spectroscopy (EDX). Based on these data, a phase diagram taking into account the sulfur concentration of the films was built. Finally, five films representative of the specific sets of samples, were selected and their electrical properties were characterized by Hall effect method.

2. Experimental details

All experiments were carried out in a cylindrical stainless steel chamber. The system was equipped with two K.J. Lesker Torus magnetron. The substrate was located in front of the two magnetron cathodes at a distance of 20 cm. More details about the deposition chamber, the magnetron cathodes and the geometry can be found in Ref. [17]. The different CuSn targets [60 at.% Cu – 40 at.% Sn ($Cu_{60}Sn_{40}$) and 50 at.% Cu – 50 at.% Sn ($Cu_{50}Sn_{50}$)] and the Zn one were sputtered in Ar–H_2S gas mixtures. These targets were sputtered with a power (P_{CuSn}) varying between 35 and 60 W, keeping constant the power applied to the Zn target (P_{Zn}) at 50 W. For the two set of experiments, the Ar–H_2S gas flow ratio and the total pressure were kept constant at 10–10 sccm and 5 mTorr, respectively.

The films were deposited on soda lime glass substrates. The elemental composition was determined by Electron Dispersive X-Ray (EDX). These measurements were performed with a Hitachi SU8020 device using an acceleration voltage of 20 kV. The Cu, Zn, Sn and S K-lines were selected for quantitative composition determination. The phase constitution of the film was measured by Raman spectroscopy using two wavelengths. First, Raman spectra were recorded by a Bruker Santerra micro-Raman with a spectral resolution of 3 cm^{-1}. A 785 nm wavelength with a power of 1 mW and a spot size of 50 μm in diameter were used. Second, Raman spectroscopy was performed using UV excitation wavelength at 325 nm thanks to a Horiba Jobin Yvon HR800UV spectrometer. After subtraction of the background, the resulting spectra were fitted by Lorentzian functions in order to identify the different phases. The films were also characterized by X-Ray Diffraction (XRD) in θ–2θ configuration using a PANalytical Empyrean system ($CuK\alpha_{1,2}$ radiation). XRD measurements were performed in order to observe the presence of species which are non-active in Raman spectroscopy. The percentage of the different phases was roughly estimated from the intensities of the main XRD peaks. Finally, five representative films were chosen and their electrical properties were characterized by Hall effect measurements using the Van der Pauw method on a Variable Temperature Hall Effect Measurement equipment (MMR Technologies).

3. Results and discussion

3.1. Characterization of the films

16 films were deposited on soda lime glass substrates varying P_{CuSn} from 35 to 60 W and using the two CuSn targets. At the same time all other experimental parameters were kept constant. The films are referenced in Table 1 with the corresponding P_{CuSn}. The 4 films deposited for the same range of P_{CuSn} and using another CuSn target composition (67–33%at. – $Cu_{67}Sn_{33}$) are added to the list (these last data are extracted from our previous paper [17]). In this section, we present the material characterization of these films in term of phase constitution and chemical composition.

All films were characterized by Raman spectroscopy using the 785 nm wavelength (λ_{785}) allowing the identification of CZTS phase in thin films because its energy is close to the optical bandgap of the CZTS [18]. The Raman spectra of the 20 films are presented in Fig. 1 where two phases can be identified: CZTS which presents peaks for 263, 288, 302, 316, 325, 338, 353, 366 and 374 cm^{-1} and SnS which presents peaks for 68, 97, 168, 190 and 220 cm^{-1} [18]. It has to be noticed that the peak at 325 cm^{-1} corresponds to the wurtzite phase of the CZTS, whereas the others are characteristics of the kesterite phase [19]. For the $Cu_{60}Sn_{40}$ target, the evolution of the phase constitution is similar than the one observed for the $Cu_{67}Sn_{33}$ target [17]. Indeed, three groups of sample can be constituted according to P_{CuSn}: low power (35 W), medium powers (40–50 W) and high powers (55 and 60 W) groups. For P_{CuSn} = 35 W, only the CZTS peaks are visible. The SnS phase starts to appear for medium power but CZTS still dominates. For higher powers the CZTS phase is not detected anymore. Using the $Cu_{50}Sn_{50}$ target, the evolution of the phase constitution is slightly different. Indeed, the SnS and CZTS phases coexist from the lowest power (P_{CuSn} = 35 W). As for the other targets, the SnS peak intensities increase with P_{CuSn}. Using this target, the phase constitution is dominated by SnS even at medium power, and for high power conditions, the only observable phase is SnS.

For all CuSn targets, it appears that the presence of SnS peaks is related to the increase of P_{CuSn}. This is shown in Fig. 2 where the relative intensities of the more intense SnS and CZTS peaks, at 220 and 338 cm^{-1}, respectively are represented according to P_{CuSn}. The relative intensities are calculated using the following equation: